

# MEASUREMENTS ON THE GOLEM TOKAMAK

MEASUREMENT LOGBOOK

Measurement guides:

Gergő Pokol

Vojtech Svoboda

Made by:

Annamária Kéri (NS89L2)

Márton Horváth (AMYK3L)

Máté Gergely Halász (ULIMI0)

Location of measurement: BME Institute of Nuclear Technology

Date of measurement:

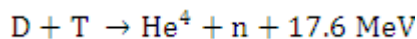
17 September 2012

## 1. Goals of the laboratory exercise

The goal of this laboratory exercise was twofold: firstly, to get a brief introduction to plasma physics and thermonuclear fusion technology, and secondly, to gain experience in remote controlled measurements.

## 2. Theoretical introduction

Energy production is a major question of sustainable development, in which thermonuclear fusion technology will certainly play a major role in the foreseeable future. The most significant of the possible fusion reactions is the D-T (deuterium-tritium) reaction, which takes place in the following form:



The problem is that this reaction becomes significant only at very high temperatures, such high that in a terrestrial vessel particles with the required temperature would escape to the wall in microseconds. The solution to this problem is given by magnetic confinement.

In a tokamak device (for the schematic structure see figure 1.) magnetic confinement is achieved by the superposition of toroidal magnetic field generated by external coils and a poloidal magnetic field generated by the toroidal plasma current induced by the transformer coil. The result is a magnetic field, in which field lines are winding helically around the torus surface. The helical structure of the magnetic surface is described by the safety factor ( $q$ ), which can be estimated at large aspect ratios by the following formula:

$$q(r, t) = \frac{r}{R} \cdot \frac{B_t(t)}{B_p(r, t)} \quad (2.1)$$

where  $r$  is minor radius, and  $R$  is the major radius of the magnetic axis,  $B_t(t)$  is the toroidal magnetic field, and  $B_p(r, t)$  is the poloidal magnetic field. The safety factor characterizes the stability of the established plasma by giving the number of  $360^\circ$  twists in the helical structure. At rational values particles arrive at the same place after performing one full round in the toroidal, thus making the distribution of kinetic energy slower, hence the created plasma will become quite unstable.

Another important global quantity related to the confined plasma is the energy confinement time, which describes the energy balance of the fusion reactor. The energy confinement time is defined as the characteristic time of energy loss:

$$\tau_E = \frac{W_{pl}}{P_{loss}} \quad (2.2)$$

where  $W_{pl}$  is the total plasma energy, and  $P_{loss}$  is the power lost. A simple threshold for self-sustained thermonuclear fusion reaction is the so-called Lawson criterion, which marks a minimum value to the product of plasma density ( $n$ ) and confinement time:

$$n \cdot \tau_E > 20 \text{ m}^{-3} \text{ s} \quad (2.3)$$

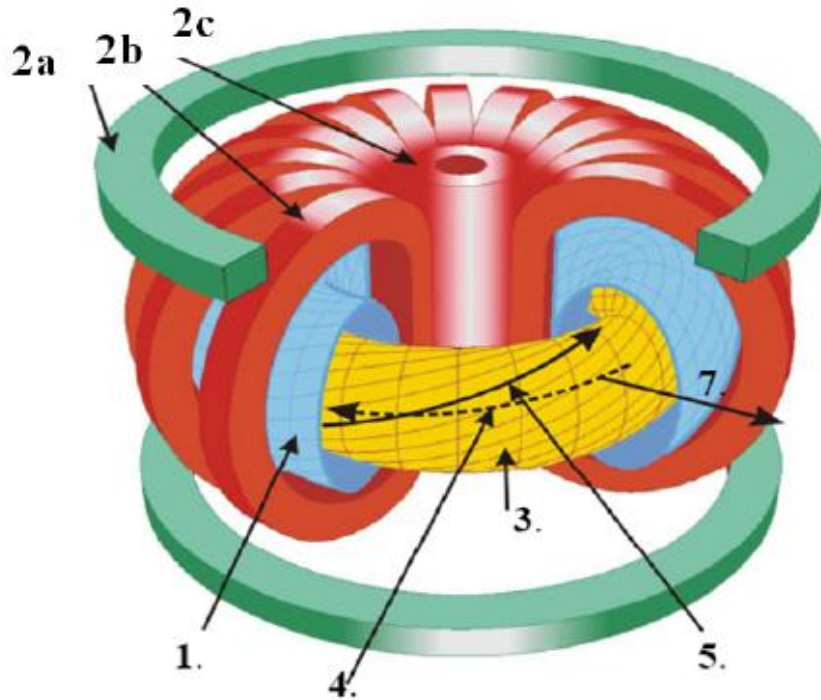


*Figure 1: Schematic structure of a tokamak device: (1) vacuum chamber, (2a) poloidal field coil / vertical field coil, (2b) toroidal field coil, (2c) transformer coil, (3) plasma, (4) plasma current, (5) magnetic field line, (7) radial direction (r)*

### 3. The GOLEM tokamak

The GOLEM tokamak is a small sized tokamak device intended for research and educational purpose, equipped with full remote control capability (figure 2.). The device has the following dimensions:

- Major radius at the magnetic axis:  $R_0 = 0.4$  m.
- Minor radius:  $r_0 = 0.1$  m.
- Radial position of the limiter:  $a = 0.085$  m.

Ignition in the GOLEM tokamak is solved by a glow discharge, and heating is provided with ohmic heating. Parameters which can be set remotely are the following:

- Toroidal magnetic field ( $B_t$ ): determined by the voltage of toroidal field capacitor banks ( $U_B$ ), range: 400-1400 V
- Toroidal electric field ( $E_t$ ): through the capacitor bank for the current drive ( $U_E$ ), range: 100-600 V
- Time delay between the triggers of the toroidal magnetic field and the current drive ( $T_{CD}$ ), range: 0-20000  $\mu$ s
- Hydrogen gas pressure ( $p_{H_2}$ ): 0-100 mPa
- Preionization: ON/OFF

Online accessible diagnostics:

- Time resolved measurement of loop voltage ( $U_l$ )
- Time resolved measurement of total toroidal current by Rogowski coil ( $I_t$ )
- Time resolved toroidal magnetic field by coil measurement ( $B_t$ )
- Time resolved measurement of plasma radiation by photodiode
- Vacuum chamber pressure ( $p_{ch}$ )
- The temperature of the vacuum chamber ( $T_{ch}$ ): estimated by room temperature

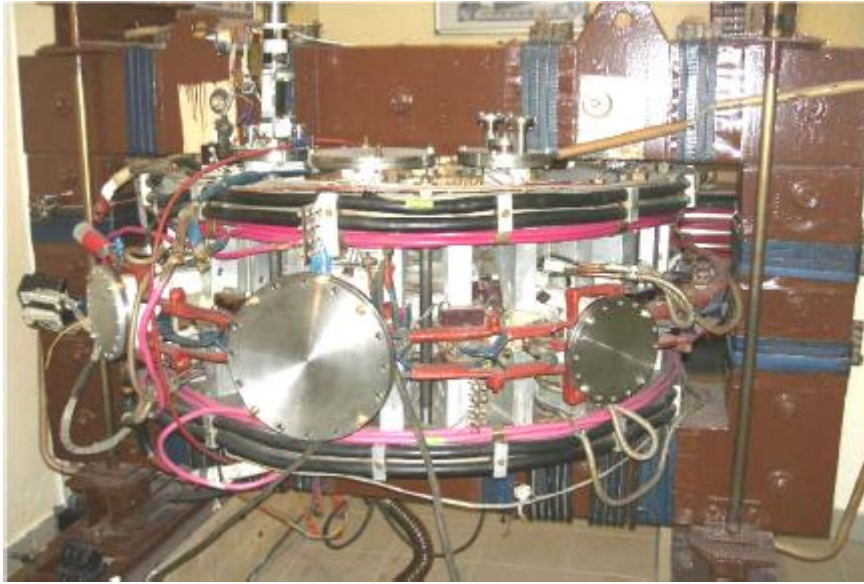


*Figure 2: Photo of the GOLEM tokamak device*

## 4. Measurement tasks

### 4.1. Determination of vacuum chamber parameters

In a vacuum shot, when no plasma is formed, it is possible to determine the resistance of the vacuum vessel because all the current measured flows in the vessel.

The loop voltage from the circuit equation is:

$$U_l(t) = R_{ch} \cdot I_{tot} + L_{ch} \frac{dI_{tot}}{dt} \quad (4.1)$$

where  $R_{ch}$  is the resistance of the chamber,  $I_{tot}$  is the total (in this case it is also the chamber) current and  $L_{ch}$  is the inductance of the chamber.

Considering the given data points, the (4.1) equation becomes an overdetermined linear equation system,  $R_{ch}$  and  $L_{ch}$  being the unknown parameters:

$$\bar{U}_l(t) = R_{ch} \cdot \bar{I}_{tot} + L_{ch} \frac{d\bar{I}_{tot}}{dt} \quad (4.2)$$

where  $\underline{U}_j$ ,  $\underline{I}_{\text{tot}}$ , and  $\underline{dI}_{\text{tot}}$  are vectors containing the corresponding values at each data point. The (4.2) equation system can be written in the following form:

$$\overline{\underline{A}}\overline{\underline{X}} = \overline{\underline{Y}} \quad (4.3)$$

where  $\underline{A}$  is a matrix made of vectors  $\underline{I}_{\text{tot}}$  and  $\underline{dI}_{\text{tot}}$ ,  $\underline{X}$  is a vector containing  $R_{\text{ch}}$  and  $L_{\text{ch}}$ , and  $\underline{Y}$  is  $\underline{U}_j$ . Assuming the rows of  $\underline{A}$  are linearly independent (which is usually true), the so-called Moore-Penrose pseudoinverse gives the least squares solution of the overdetermined problem:

$$\overline{\underline{X}} = (\overline{\underline{A}^T \underline{A}})^{-1} \overline{\underline{A}^T \underline{Y}} \quad (4.4)$$

We summarized the fitted parameters in table I. As an example, the result of the least squares regression for shot number xxxx can be seen on figure 4.1.

Table I.: Vacuum chamber parameters

Shot no.	R ( $\Omega$ )	L (H)
Shot 1	$9.97 \cdot 10^{-3}$	$1.29 \cdot 10^{-7}$
Shot 2	$9.93 \cdot 10^{-3}$	$2.55 \cdot 10^{-8}$
Shot 3	$1.05 \cdot 10^{-2}$	$3.76 \cdot 10^{-7}$
Shot 4	$1.01 \cdot 10^{-2}$	$1.64 \cdot 10^{-7}$
Average	$1.01 \cdot 10^{-2}$	$1.74 \cdot 10^{-7}$

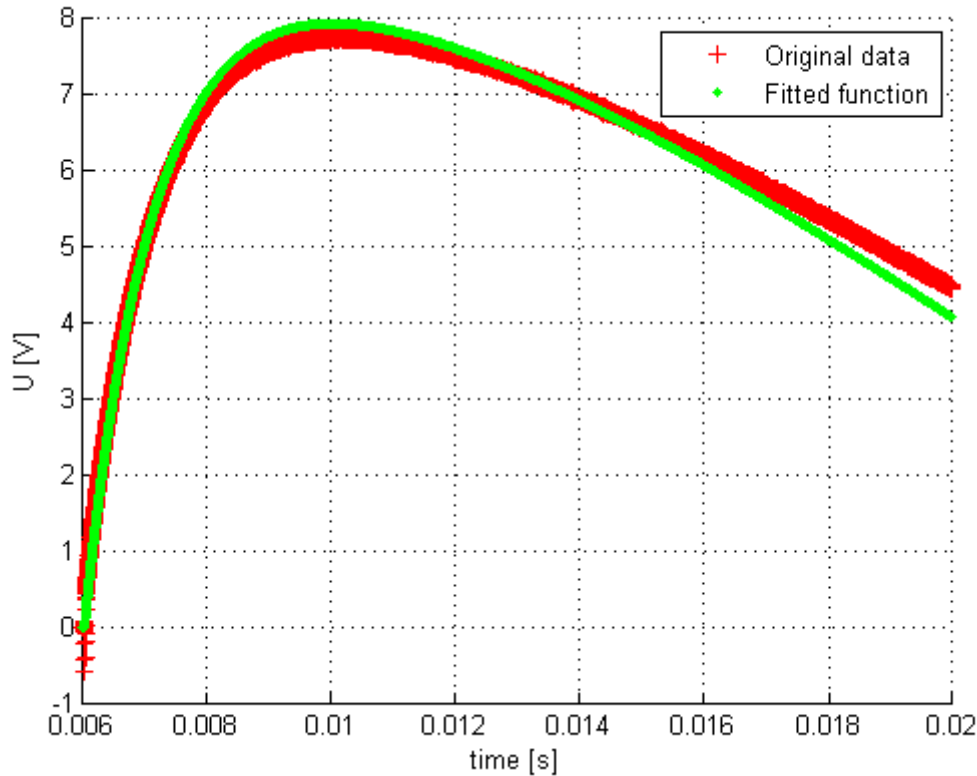


Figure 4.1.: The result of the least-squares regression for shot no. 9858

## 4.2. Plasma brakedown

After vacuum measurements H<sub>2</sub> gas was let into the chamber and pre-ionized to produce plasma. Changing the values of the parameters the properties of the plasma were studied.

First plasma break down (the critical value for mass ionization) was searched therefore two discharge parameter, the maximum loop voltage ( $U_l$ ) and the gas pressure ( $p_{ch}$ ) was adjusted for several values.

During the measurements, we found out, that the H<sub>2</sub> valve did not work the way, we expected, because, in cases, when we attempted to let gas quantity from the lesser end of the scale, the valve showed nonlinear characteristics in the gas inlet as a function of the set value of the gas inlet with remote control. The difference between the planned and the realised inlet was sometimes more than 100% percent. On the other hand, at the middle or end of the available scale, this difference was less than 5%. To determine the critical line separating breakdown and non-breakdown shots were concentrated in this domain.

The measurement results are summarized in table II.:

*Table II.: Plasma brakedown*

Measurement no.	$U_{CD}$ (V)	$p_{H_2}$ (mPa)	$U_B$ (V)	$T_{CD}$ ( $\mu$ s)	Plasma
9860	500	4.43	600	1000	yes
9861	500	2.74	600	1000	no
9862	500	4.54	600	1000	yes
9863	500	16.74	600	1000	yes
9864	500	40.92	600	1000	no
9865	500	67.65	600	1000	no
9866	500	34.96	600	1000	no
9867	500	30.10	600	1000	yes
9868	100	3.15	600	1000	no
9869	100	5.35	600	1000	no
9870	100	15.92	600	1000	no
9871	100	40.25	600	1000	no
9872	100	40.30	600	1000	no
9873	100	84.20	600	1000	no
9874	300	12.35	600	1000	yes
9875	300	7.41	600	1000	yes
9876	300	4.06	600	1000	yes
9877	300	2.92	600	1000	no
9878	200	6.05	600	1000	no
9880	200	19.96	600	1000	no
9881	250	19.73	600	1000	no
9882	250	49.20	600	1000	no
9883	600	12.07	600	1000	yes
9884	600	5.25	600	1000	yes
9885	600	49.58	600	1000	yes
9886	600	35.23	600	1000	yes
9888	600	20.00	600	1000	yes

On figure 4.2. we summarized the results of the 29 discharges, where we measured the presence of the plasma as a function of  $U_{CD}$  and the  $H_2$  gas pressure.

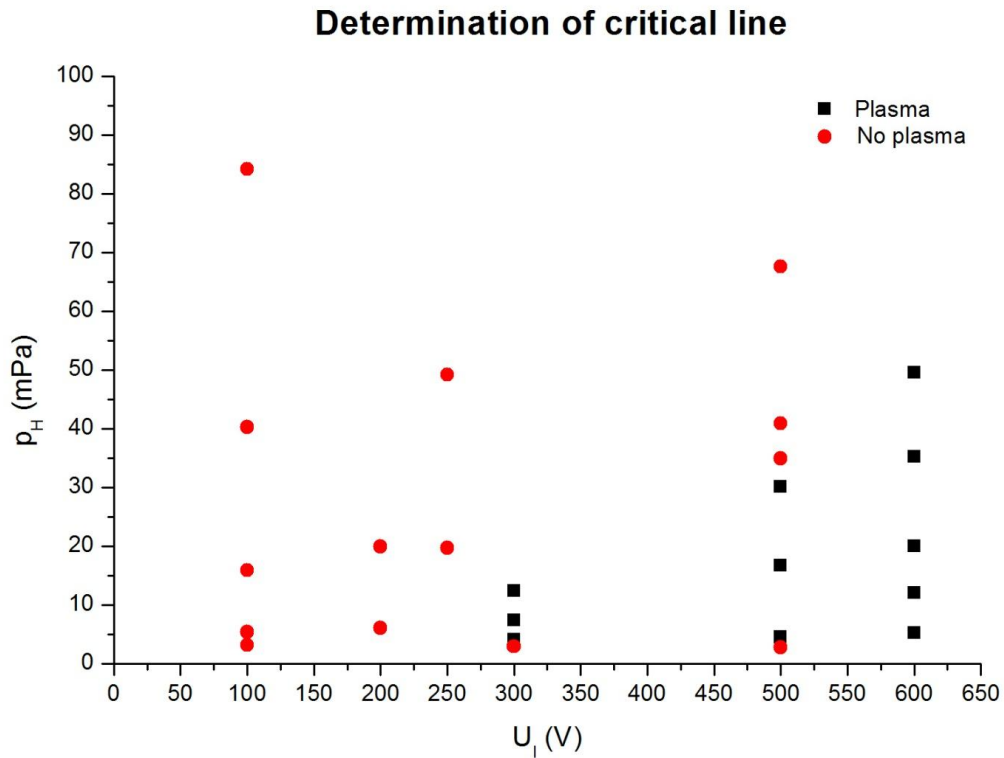


Figure 4.2.: Determination of critical line

#### 4.3. Estimation of the main plasma parameters

At this point, we investigated the effects of the different parameters, on the performance of the discharge. Therefore our aim was to achieve the highest central temperature, plasma energy and confinement time.

At first, we attempted to find the settings to perform maximum central temperature. At first, we assumed, that this will be the case, when we have maximum electric field, (which we could set by changing the value of the capacitor bank for the current drive ( $U_E = U_{CD}$ )), with the least amount of  $H_2$  gas possible to form plasma.

Our measurements however show, that the maximum central temperature was achieved under the conditions, where

- Shot N.o.:9891
- $U_{CD}=600V$
- $P_{H_2}=3,74mPa$
- $U_B=600V$
- $T_{CD}=1000\mu s$
- $T_e \text{ max}=574350 K$

Which was not achieved within the shots, designed to achieve a maximum from the mentioned parameters before. But it was either the maximum  $U_{CD}$  set with the minimum  $H_2$  inlet, when plasma was created.

After the last part, we did not have enough shots left to use them on to finding the highest plasma energy and confinement time. Nonetheless we searched for them amongst our shots, the results were the following:

- The highest plasma energy was achieved under the conditions, where
- Shot N.o.:9885
- $U_{CD} = 600V$
- $P_{H_2} = 35,23mPa$
- $U_B = 600V$
- $T_{CD} = 1000\mu s$
- $W_{pl,max} = 1,8353 J$

These conditions mean, that during this shot, maximum electric field was used, with relatively high plasma pressure. In fact, there was only one shot, where we used higher  $H_2$  pressure with the same  $U_{CD}$  and still achieved plasma, but it was a borderline case.

The shot mentioned above was n.o. 9885, where we were able to create plasma, but for a much shorter period, than the other cases. Our evaluating algorithms couldn't run on this case, because the plasma current was under 500A, the plasma temperature was about 50000K.

The highest confinement time was at the same shot as the highest plasma energy, which is not a surprising result, because if the power loss doesn't change between too large borders, where we have, the maximum power, there will it remain for the longest time.

#### 4.4. Plasma current

Our first measurement task was to estimate the plasma current. A simple electrical model is a circuit, in which the LR circuits of the plasma and the vacuum chamber are connected in parallel with a time-varying voltage source, the loop voltage ( $U_l$ ). Knowing the inductivity and resistance of the vacuum chamber – which are constant values -, the plasma current can be calculated using the following circuit equations:

$$U_l(t) = R_{ch} \cdot I_{ch}(t) + L_{ch} \cdot \frac{dI_{ch}(t)}{dt} \quad (4.5)$$

$$U_l(t) = R_{pl}(t) \cdot I_{pl}(t) + L_{pl} \cdot \frac{dI_{pl}(t)}{dt} \quad (4.6)$$

$$I_{tot}(t) = I_{pl}(t) + I_{ch}(t) \quad (4.7)$$

where  $U_l(t)$  is the loop voltage,  $R_{ch}$  and  $L_{ch}$  are in order the vacuum chamber resistivity and inductivity,  $R_{pl}$  and  $L_{pl}$  are the plasma resistivity and inductivity, and  $I_{tot}$  is the total current. As seen in chapter 4.1., the inductivity of the vacuum chamber is close to zero, thus we can estimate the (4.5) equation in the following form:

$$U_l(t) = R_{ch} \cdot I_{ch}(t) \quad (4.8)$$



This way the chamber current can be calculated by dividing the loop voltage by the chamber resistance at each sampling point. The value of the plasma current can be given using equation (4.7) by subtracting the chamber current from the total current:

$$I_{pl}(t) = I_{tot}(t) - I_{ch}(t) \quad (4.9)$$

Now, as we know the time-varying plasma current, we can use (4.6) to calculate the plasma resistivity using the assumption  $L_{pl} \approx 0$  H:

$$R_{pl}(t) = U_1(t)/I_{pl}(t) \quad (4.10)$$

On figures 4.3. and 4.4. we displayed the time dependence of the plasma current, and on figures 4.5. and 4.6. we displayed the time dependence of the plasma resistivity for shots n. o. 9874 and 9867. We only displayed data in the time interval, where plasma current was greater than 500 A. The resistivity is mainly influenced by the temperature of the plasma, hence resistivity becomes very large at the end of measurements, when the plasma cools down.

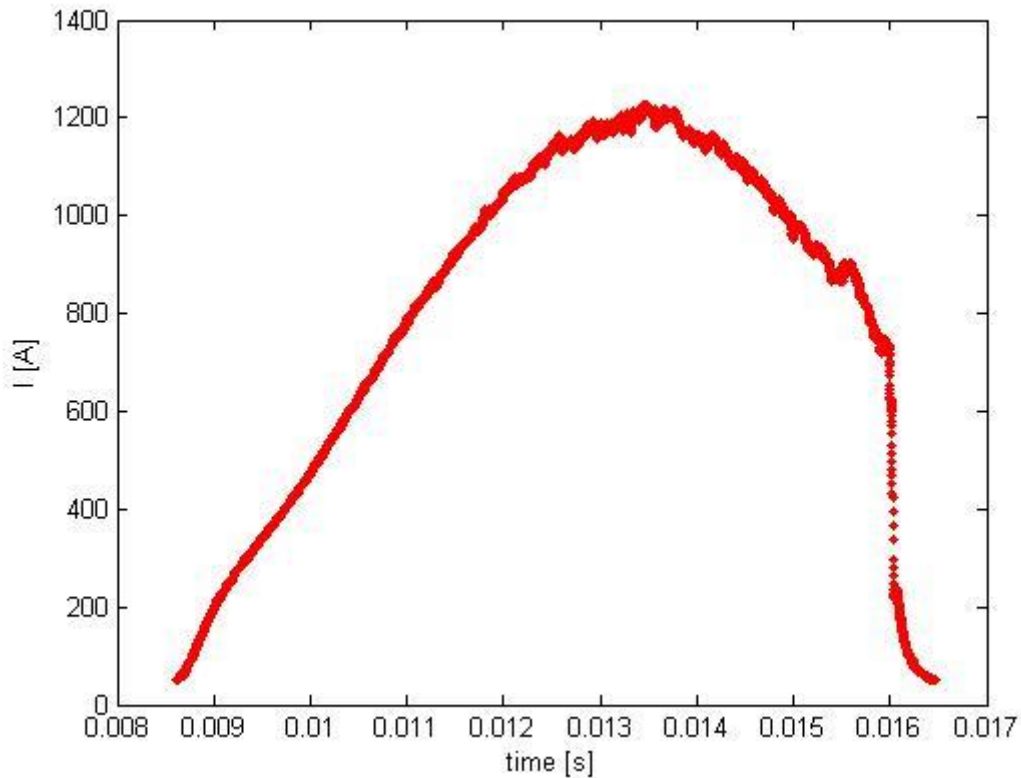


*Figure 4.3.: Time dependence of the plasma current for shot number 9874*

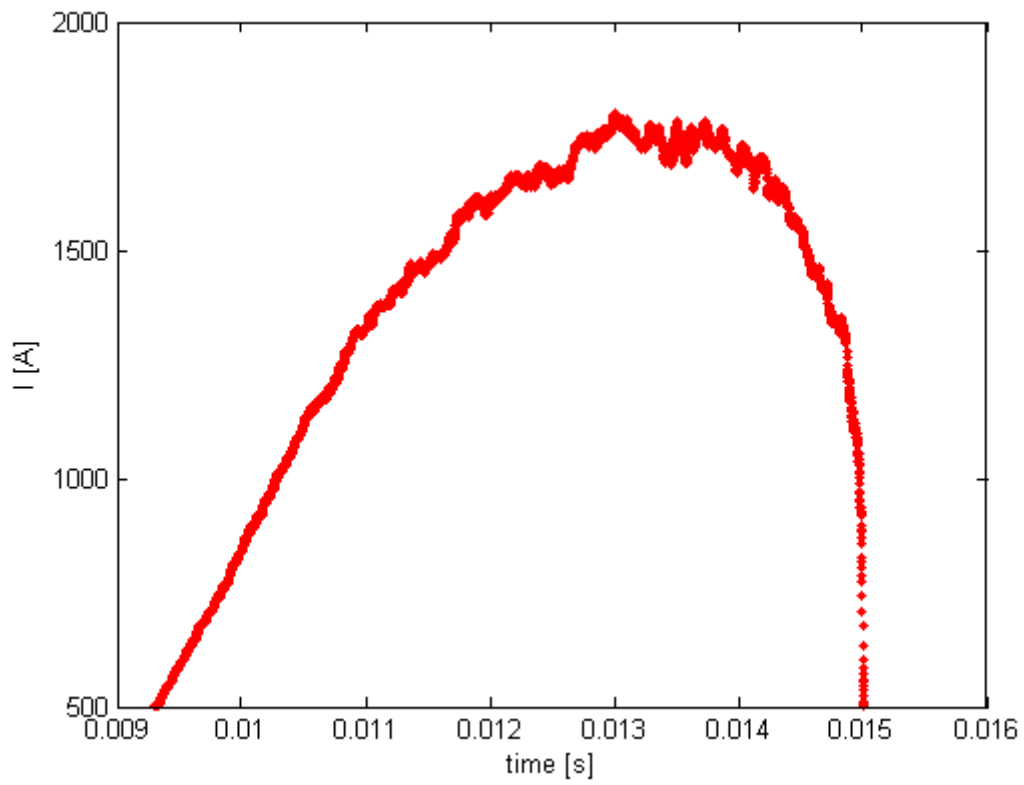


Figure 4.4.: Time dependence of the plasma current for shot number 9867

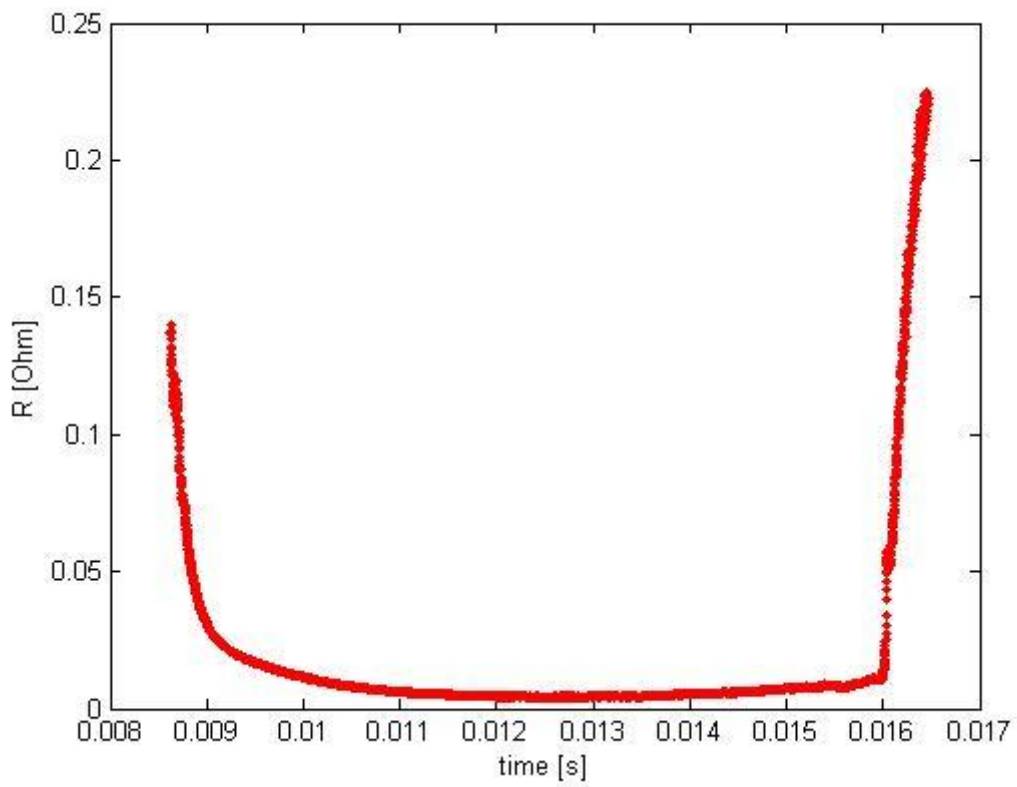


Figure 4.5.: Time dependence of the plasma resistivity for shot number 9874

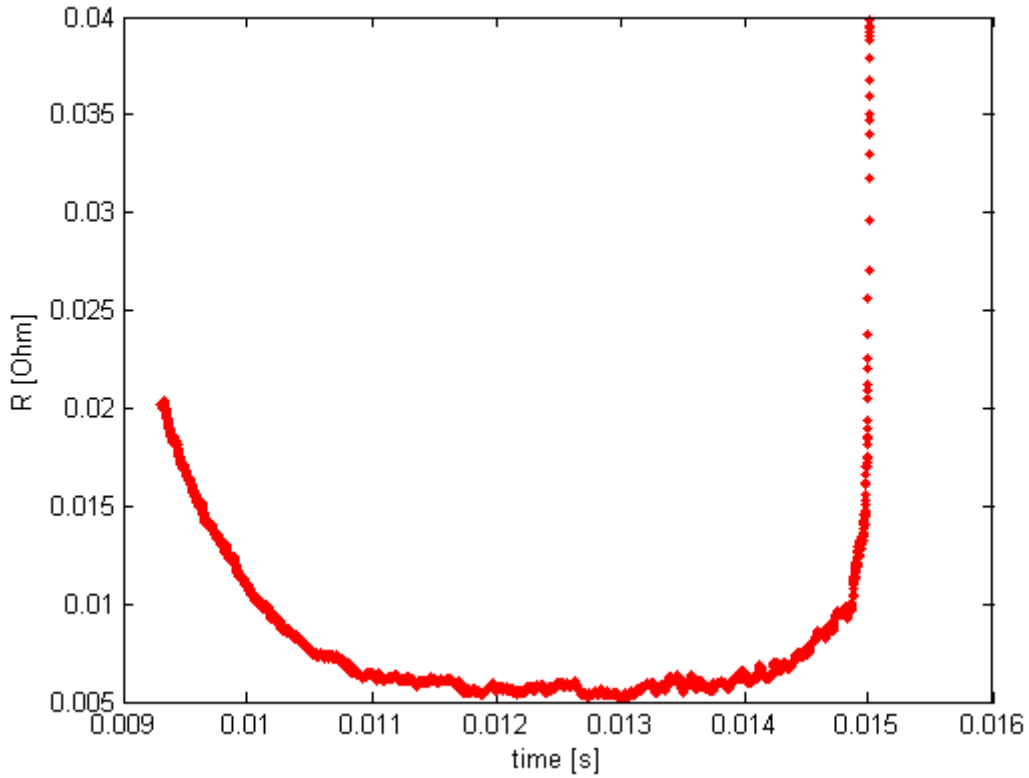


Figure 4.6.: Time dependence of the plasma resistivity for shot number 9867

#### 4.5. Plasma heating power

In the GOLEM tokamak, the plasma heating is results from ohmic porcess. Where we can calculate the heating power from the following formula:

$$P_{OH}(T) = R_{PL}(t) \cdot I_{PL}^2(t) \quad (4.11)$$

where  $R_{pl}(t)$  and  $I_{pl}(t)$  are in order the plasma resistance and current. The maximum heating power we used was  $P_{OH} = 46862$  W, at shot n.o.: 9883.

#### 4.6. Central electron temperature

The resistivity of the ionized plasma depends on the electron temperature. The profile of the electron temperature as a function of described by the following formula:

$$T_e(r, t) = T_{e0}(t) \cdot \left(1 - \frac{r^2}{a^2}\right)^2 \quad (4.12)$$

Where  $t$  is the time and  $r$  is minor radius, and the central electron temperature is the following:

$$T_{e0}(t) = \left( \frac{R_0}{a^2} \cdot \frac{8Z_{eff}}{1544} \cdot \frac{1}{R_{pi}(t)} \right)^{2/3} \quad (4.13)$$

Where  $R_{pl}$  is the resistivity of the plasma,  $Z_{eff}$  is the effective charge, radial position of the limiter. We displayed the time dependence of the central electron temperature during shot no. 9874 on figure 4.7.

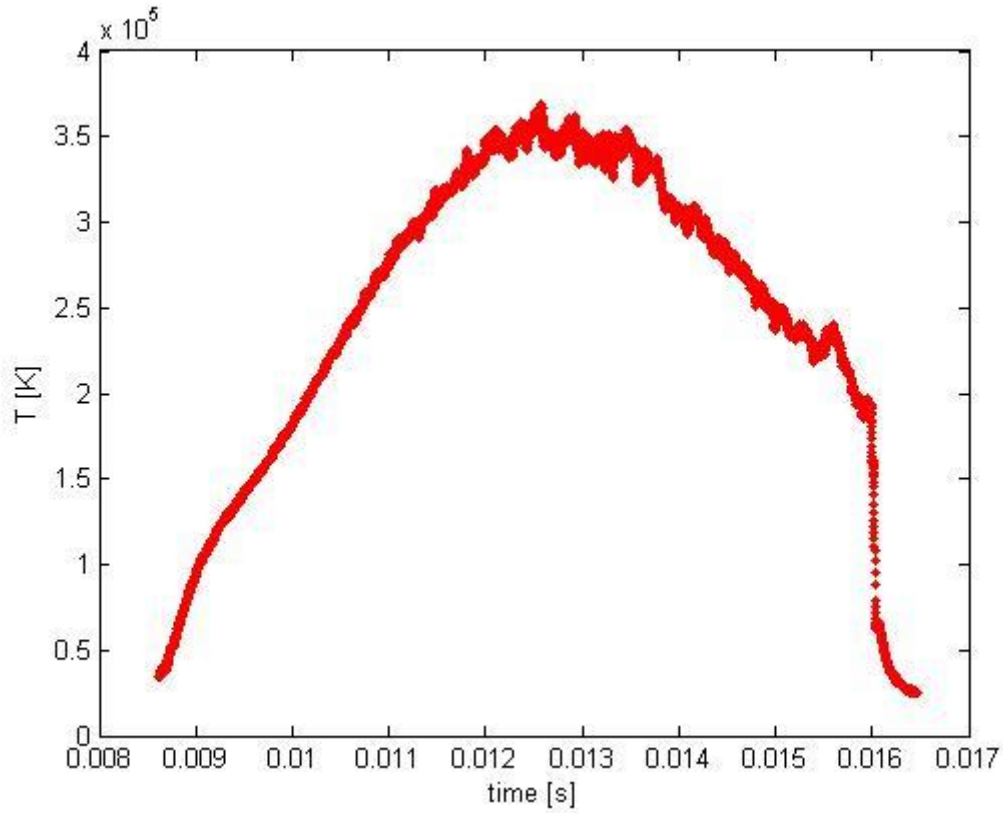


Figure 4.7.: Time dependent central electron temperature of shot no. 9874

#### 4.7. Electron density

We use the formula given down below to estimate the order of magnitude of the electron density. We use the fact, that the  $H_2$  temperature reaches the equilibrium with the chamber wall, so we can use the ideal gas law to estimate the electron density:

$$n_{avr} = \frac{2 \cdot P_{ch}}{k_B \cdot T_{ch}} \quad (4.14)$$

It is a rough estimation, due to plasma wall interaction, and due to the fact, that in GOLEM, the plasma is not fully ionized.

#### 4.8. Plasma energy

Based on the ideal gas law, the total energy content of the plasma can be calculated from the assumed temperature profile, the average density and volume, in knowledge that the magnetic field reduces the degree of freedom of the particles to two:

$$W_{pl}(t) = V \cdot \frac{n_{avr} \cdot k_B \cdot T_{e0}(t)}{3} \quad (4.15)$$

We measured the maximum plasma energy during shot no. 9886, with the value of 1,8353 J. However, uncertainty of this formula – which comes from the uncertainty of the estimation of density – makes it only good for an order of magnitude estimate.

We displayed the time dependent plasma energy of shot no. 9867 on figure 4.8. as an example.

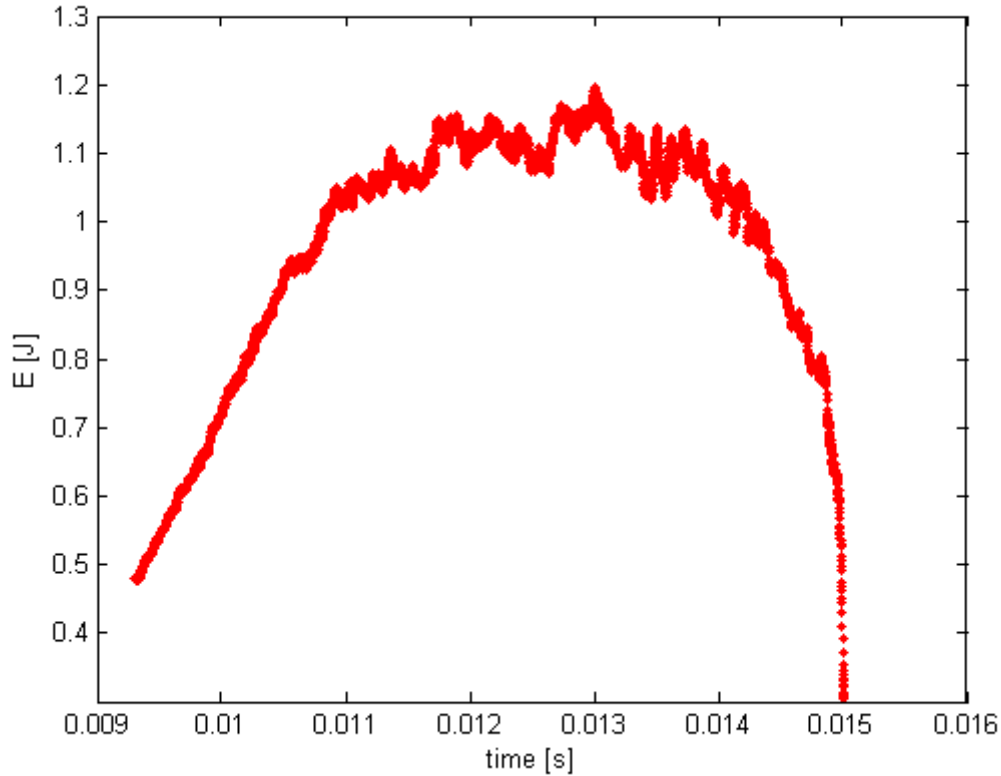


Figure 4.8.: Time dependent plasma energy of shot no. 9867

#### 4.9. $q = 2$ disruptions

The task was to reach the value of 2 with the edge safety factor defined by equation (4.15).

$$q(a, t) = \frac{a^2 2B_t(t) \cdot \pi}{R_0 \mu_0 \cdot I_{pl}(t)} \quad (4.15)$$

In this case the plasma becomes instability and a discharge terminating occurs. To monitor the successful of the shot Hugil diagrams was plotted during evaluation of the measurements. On the diagram the inverse of the edge safety factor was plotted with respect to Murakami parameter (normalized density). Murakami parameter can be calculated by equation (4.16):

$$\frac{n_{avg} \cdot R_0}{B_t} \quad (4.16)$$

where  $n_{avg}$  is the electron density,  $R_0$  the major radius at the magnetic axis and  $B_t$  toroidal magnetic field.

To achieve the aim plasma current was increased as large as possible and toroidal magnetic field was reduced. Unfortunately the measurement was not successful because at the value of the minimum toroidal field plasma cannot be created. The reason is that the value of the time delay cannot be increased over 20,000  $\mu\text{s}$ . The best result to achieve the required value of the edge safety factor can be seen on Figure 4.9.

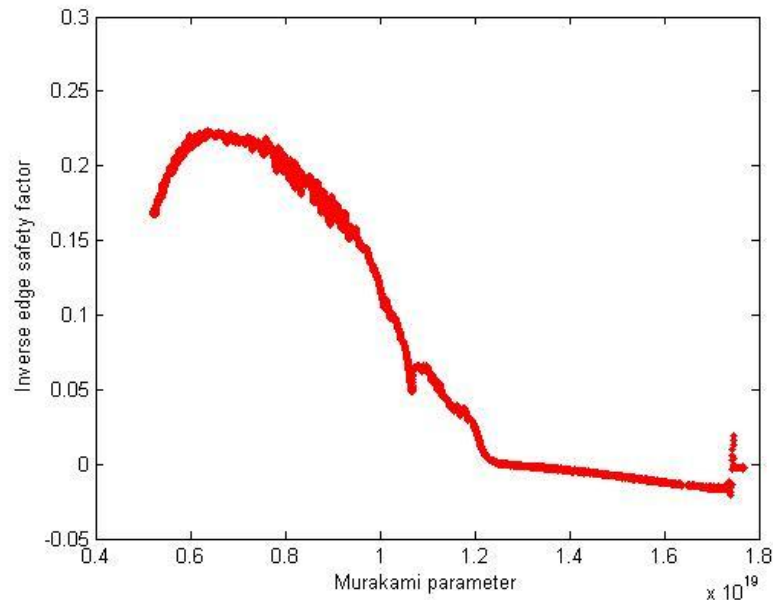


*Figure 4.9.: Hugil digram at the maximum value of the plasma current and the minimum value of the toroidal magnetic field*

The results of the previous shots were also plotted on Hugil diagrams to check that in none of them was the safety factor under value of 2.

## 5. Conclusion

During the laboratory exercise, we got a brief introduction to plasma physics and fusion technology, and gained experience in remotely controlled measurements. In the first task we successfully determined the parameters of the vacuum chamber, specifically the resistivity and inductivity of the chamber. In the next few tasks we successfully created plasma and measured its describing parameters, such as the plasma current, resistivity, the central electron temperature of the plasma, central plasma temperature, and plasma energy etc. We learned much about the basics of thermonuclear fusion, with special attention to tokamak devices and learned about co-working with foreign laboratories.

## Acknowledgements

We would like to thank Dr. Vojtech Svoboda for the opportunity and the help he provided us during the laboratory exercise. We would also like to thank Dr. Gergő Pokol and László Horváth for their assistance and advices.

## Appendix

Table III: Summary of the parameters of the shots

Shot N.o.	$U_{CD}$	P	Plasma	$U_B$	$T_{CD}$
9859	500	8,45	1	600	1000
9860	500	4,43	1	600	1000
9861	500	2,74	0	600	1000
9862	500	4,54	1	600	1000
9863	500	16,67	1	600	1000
9864	500	0,97	0	600	1000
9865	500	67,65	0	600	1000
9866	500	34,96	0	600	1000
9867	500	30,1	1	600	1000
9868	100	3,15	0	600	1000
9869	100	5,35	0	600	1000
9870	100	15,92	0	600	1000
9871	100	40,45	0	600	1000
9872	100	40,3	0	600	1000
9873	100	84,2	0	600	1000
9874	300	12,35	1	600	1000
9875	300	7,41	1	600	1000
9876	300	4,06	1	600	1000
9877	200	2,92	0	600	1000
9878	200	6,05	0	600	1000
9879	error	16,99	*	600	1000
9880	200	19,96	0	600	1000
9881	250	19,73	0	600	1000
9882	250	49,2	0	600	1000
9883	600	12,07	1	600	1000
9884	600	5,25	1	600	1000
9885	600	49,58	1	600	1000
9886	600	35,23	1	600	1000
9887	600	20,51	1	600	1000
9888	600	19,21	1	600	1000
9889	600	7,19	1	600	1000
9890	600	0,86	0	600	1000
9891	600	3,74	1	600	1000
9892	600	1,83	0	1400	1000
9893	600	1,25	0	1000	1000
9894	600	1,08	0	600	1000
9895	600	1,06	0	1000	16000
9896	600	1,72	0	1000	16000
9897	600	2,33	0	600	1000
9898	600	5,6	1	600	1000

9899	600	9,63	1	1000	16000
9900	600	7,85	0	1000	16000
9901	600	8,48	0	100	500
9902	600	18,14	1	400	500

\*the files containing the results of the measurement were damaged, so that the results were could not be evaluated.

*Table IV.: Advanced shot infirmation data (in cases, where plasma was created)*

*(highlighted cells represent the maximum values of the current column)*

Shot N.o.	R <sub>p</sub> max	I <sub>p</sub> max	P <sub>OH</sub> max	T <sub>e</sub> max	n <sub>avr</sub> max	W <sub>pl</sub> max	τ <sub>E</sub>
9859	0,0429	2877	30755	451260	4,0821E+18	0,4834	4,28E-05
9860	0,0444	2906,9	30564	476560	2,1401E+18	0,2676	4,91E-06
9862	0,0448	2968,4	31026	493460	2,1932E+18	0,2840	2,01E-05
9863	0,0452	2837,5	29719	472040	8,0531E+18	0,9975	2,76E-05
9867	0,0398	1801,1	18384	313690	1,4541E+19	1,197	6,00E-05
9874	0,0191	1225,4	7297,6	369360	5,9662E+18	0,5793	4,64E-05
9875	0,0214	1762,1	10824	515580	3,5797E+18	0,4843	3,85E-05
9876	0,0215	1830,2	11143	556060	1,9614E+18	0,2862	2,22E-05
9883	0,0536	3542,4	46862	475730	5,8309E+18	0,7279	1,28E-05
9884	0,0545	3493,2	44099	482520	2,5362E+18	0,3211	6,13E-06
9886	0,0553	2962,2	37688	410950	1,7019E+19	1,8353	8,18E-05
9887	0,0199	3457,1	43038	465830	9,9082E+18	1,2112	2,59E-05
9888	0,056	3498,5	44345	481150	9,2802E+18	1,1717	2,33E-05
9889	0,0567	3645,1	44464	519660	3,4734E+18	0,4737	2,02E-06
9891	0,0581	3655,2	45461	574350	1,8068E+18	0,2723	4,84E-06
9898	0,0558	3598,5	45168	487900	2,7053E+18	0,3464	1,97E-05
9902	0,0618	3180	41328	452830	8,7633E+18	1,0413	5,93E-05
Max	0,0618	3655,2	46862	574350	1,7019E+19	1,8353	8,18E-05